Land Degradation Detection Using Remote Sensing and GIS for Hambantota District in Sri Lanka

M.H.R.M. De Silva

May, 2017

Land Degradation Detection Using Remote Sensing and GIS for Hambantota District in Sri Lanka

by

M.H.R.M. De Silva
FG 506

Thesis submitted to the Faculty of Geomatics, Sabaragamuwa University of Sri Lanka in partial fulfilment of the requirements for the degree of Bachelor of Science Surveying Science, Specialisation: Photogrammetry and Remote Sensing

Thesis Assessment Board

Thesis Advisors Ms. I.A.K.S. Illeperuma

Thesis Examiners Dr. H. Divithure

FACULTY OF GEOMATICS, SABARAGAMUWA UNIVERSITY OF SRI LANKA

Disclaimer

This document describes work undertaken as part of a programme of study at the Faculty of Geomatics, Sabaragamuwa University of Sri Lanka. All views and opinions expressed therein remain the sole responsibility of the author, and do not necessarily represent those of the institute.

DECLARATION

We do hereby declare that the work reported in this dissertation was exclusively carried out by us under the supervision of Ms. I.A.K.S. Illeperuma. It describes the results of our own independent research except where due reference has been made in the text. No part of this dissertation has been submitted earlier or concurrently for the same or any other degree.

Signature of the candidate:

…… Date: ……..

M.H.R.M. De Silva

Signature of the Supervisor

…… Date: ……..

Ms. I.A.K.S. Illeperuma

Signature of the Dean

…… Date: ……

Dr. H.M.I. Prasanna

Abstract

Land degradation and desertification has been ranked as a major environmental and social issue for the coming decades. Thus, the observation and early detection of degradation is a primary objective for a number of scientific and policy organizations. The studies on the degradation have become a timely topic.

This study aimed at monitoring, mapping, and assessing the land degradation in the Hambantota district in Sri Lanka with remote sensing and GIS methods. The region has significant development over recent years. Four vegetative, build up and water indices related to land degradation were applied to two Landsat ETM+ and OLI imageries to assess the extent of land degradation for the study area during the period from 2005 to 2013. A computerized land degradation severity assessment was adopted using ERDAS Imagine 9.1 and ARC Map 10.1 environments to process, manage, and analysis the raster and thematic datasets. The indices used in this research are: The Normalized Difference Vegetation Index "NDVI", The Normalized Differential Water Index "NDWI", The Normalized Difference Build up Index "NDBI", and Normalized Differential Sand Dune Index "NDSDI". The results showed a clear deterioration in vegetative cover (224.834 km^2), an increase of sand dune accumulations (141.215 km^2), and Build up area (83.732 km^2), of the total study area. In addition, a decrease in the water body area was detected (30.639 km^2). Sand dunes accumulations had increased in the total study area, with an annual increasing expansion rate is 2.206 $km^2 year^{-1}$ during the eight years covered by the study. The land degradation risk in the study area has increased annually by 32.409% during the study period.

This study finds reveals that most of the divisional secretariat areas in the study area are exposed to a serious risk of land degradation and drought water bodies and the study area is now under a risk of complete degradation by next 300 years. Finally the statistical analysis of the results indicated that the land degradation rate of the study area is shows a similar variation pattern with the water bodies decreasing rate in the area.

KEY WORDS: Land degradation, Landsat, NDVI, NDWI, NDBI, NDSDI

Acknowledgements

I take this opportunity to express my special thanks to the people who helped and encouraged me during the challenging and tough time of this research work.

My deepest sense of gratitude is expressed to my supervisor Ms. I.A.K.S. Illeperuma; Senior Lecturer, Faculty of Geomatics, Sabaragamuwa University of Sri Lanka for her precious guidance, positive encouragement and continuous support throughout the study. Madam, I highly appreciate your constructive supports, suggestions, valuable comments, and patients. It is a great opportunity and proud privilege for me to be your student.

Then I would like to thank Dr. D.R. Welikanna; Senior Lecturer, Faculty of Geomatics, Sabaragamuwa University of Sri Lanka, Coordinator of this research program for supplying necessary arrangements in great manner to carry out the task successfully.

Also I would very much owe to express deepest gratitude and sincere appreciation towards to Dr. H.M.I. Prasanna, Dean of the Faculty of Geomatics, Sabaragamuwa University of Sri Lanka and all the Lecturers, Demonstrators of the Faculty of Geomatics, Sabaragamuwa University of Sri Lanka for the contribution and for the support to succeed this thesis, for organizing and making schedules to conduct our final year thesis in good manner.

I would like to thank my parents for their unconditional love. Thank you Amma, Thaththa and my brothers and a sister for your inspiration and letting me fly. It's because of you I'm standing here.

Last but not the least; I would like to thank all my friends specially Prasadi for giving their support and contribution for the success of this study.

Table of Contents

List of Figures

List of Tables

List of Acronyms

DEM	Digital Elevation Model
DN	Digital Number
ETM+	Enhanced Thematic Mapper Plus
GIS	Geographical Information System
NDBI	Normalized Difference Building Index
NDSDI	Normal Difference Sand Dune Index
NDVI	Normalized Difference Vegetation Index
NDWI	Normal Difference Water Index
OLI	Operational Land Imager
RS	Remote Sensing
SLC	Scan Line Corrector
TIRS	Thermal Infrared Sensor
TM	Thematic Mapper
TOA	Top of Atmosphere
USGS	United States Geological Survey

1. Introduction

1.1. Background

Land degradation is temporarily or permanently lowering the productive capacity of a land (UNEP, 1992b), is increasing in severity and extent in many parts of the world, with more than 20% of all cultivated areas, 30% of forests and 10% of grasslands undergoing degradation (Bai et al., 2008). Millions of hectares of land per year are being degraded in all climatic regions. It is estimated that 2.6 billion people are affected by land degradation and desertification in more than a hundred countries, influencing over 33% of the earth´s land surface (Adams and Eswaran, 2000).

Land degradation is a complex group of surface processes; wind erosion, water erosion, soil compaction, salinization and soil water-logging. Land degradation temporarily or permanently lower the productive capacity of land (UNEP, 1992b). It is one of the most serious ecological problems faced by the globe today. It is estimated that the issue is affecting more than a hundred countries and the effect is notably significant in dry lands (Adams et al., 2000; UNEP, 1997 and Dobie, 2001). However, according to many experts opinions that the problem is variable, discontinuous in nature and can have many socio-economic impacts (Mortimore, 1998).

Land degradation leads to a significant reduction of the productive capacity of land. Human activities contributing to land degradation include unsustainable agricultural land use, poor soil and water management practices, deforestation, removal of natural vegetation, frequent use of heavy machinery, overgrazing, improper crop rotation and poor irrigation practices. Natural disasters including drought, floods and landslides are also factors that facilitate this process. Not only these factors but also political stability and socio-economic reasons such as marketing, human health, institutional support and poverty can cause to land degradation.

The consequences of land degradation are reduction of the productive capability of the land, creating socio-economic problems including uncertainty in food security, migration, limitation of the development and damaging the ecosystems. On the other hand degraded land is costly to reclaim and, if severely degraded, may no longer provide a range of ecosystem functions

and services with a loss of the goods and many other potential environmental, social, economic and non-material benefits that are critical for society and development.

When degradation becomes irreversible, then desertification appears. Desertification is land degradation in arid, semi-arid and dry sub-humid areas resulting from adverse human impact (UNEP, 1992b). Therefore it is important to assess and monitor the land degradation.

Remote sensing has been proven as a valuable tool for assessment and monitoring of degradation (Ostir K et al., 2003; Bastin GN et al., 1993; Pickup G et al., 1998 and Lacaze B., 2004). It collects multispectral, multi-resolution and multi-temporal data, and turns them into information valuable for understanding and monitoring land use changes.

1.1.1. Definition of some common types of Land Degradations

There are different types of land degradation in world. Such as Soil degradation, Forest degradation and Water degradation.

1.1.1.1. Soil Degradation

Soil degradation is the decline in soil quality caused by its improper use, usually for agricultural, pasturage, industrial or urban purposes. It is a serious global environmental problem and may be exacerbated by climate change. It encompasses physical, chemical and biological deterioration. Examples of soil degradation include loss of organic matter, decline in soil fertility, decline in structural condition, erosion, adverse changes in salinity, acidity or alkalinity, and the effects of toxic chemicals, pollutants or excessive flooding (Office of Environment and heritage, 2015).

Figure 1-1: Soil Degradation

1.1.1.2. Forest Degradation

Forest degradation is a process leading to a 'temporary or permanent deterioration in the density or structure of vegetation cover or its species composition'. It is a change in forest attributes that leads to a lower productive capacity caused by an increase in disturbances.

The time-scale of processes of forest degradation is in the order of a few years to a few decades. For the purpose of having a harmonized set of forest and forest change definitions, that also is measurable with conventional techniques, forest degradation is assumed to be indicated by the reduction of canopy cover and/or stocking of the forest through logging, fire, wind felling or other events, provided that the canopy cover stays above 10%. In a more general sense, forest degradation is the long-term reduction of the overall potential supply of benefits from the forest, which includes wood, biodiversity and any other product or service (Manual on deforestation, degradation, and fragmentation using remote sensing and GIS, Tejaswi G., March 2007).

Figure 1-2: Forest Degradation

1.1.1.3. Water Degradation

Water degradation is the pollution of water bodies such as lakes, rivers, oceans, aquifers and groundwater. This form of environmental degradation occurs when pollutants are directly or indirectly discharged into water bodies without considerable treatment to remove harmful compounds. Also it is a "renewable" resource that provides essential services, is constantly restored by the hydrologic cycle, and can be degraded when used or altered faster than it can be replenished. Due to these degradations water becomes harmful to the environment or organisms, including humans, by which the usefulness of the water resource is in some way reduced. It affects the entire biosphere – plants and organisms living in these water bodies.

Figure 1-3: Water Degradation

1.1.2. Land Degradation in Sri Lanka

It is widely accepted that land degradation is one of the most critical problems affecting the future economic development in Sri Lanka. The demands of a rapidly expanding population has set up pressures on the island's natural resources and these in turn have resulted in a high level of environmental degradation. The more important manifestations are heavy soil losses; high sediment yields; soil fertility decline and reduction in crop yields; marginalization of agricultural land; salinization; landslides and deforestation and forest degradation (National Report on Desertification / Land Degradation in Sri Lanka, 2000).

According to the UN Convention to Combat Desertification (UNCCD), there are no any desert areas defined in Sri Lanka. But several parts of the country experience serious droughts and land degradation. Hence, many laws, policies as well as programs and projects have been formulated and they are under the implementation. Under them, National Environmental policy, Draft National Land Use policy and National Watershed Management policy directly address the issue of land degradation (Review of Policies Related to Land Degradation in Sri Lanka, Abhayarathne S.G., 2007).

1.2. Research Problem

It has been estimated that nearly one third of the land in Sri Lanka is subjected to soil erosion and approximately 12,500 square miles are vulnerable to landslides. Apart from these things in recent years the country experienced frequent droughts. Droughts had very serious negative impact on the economic and social life of the country and also the natural forest cover in the country which stood at 80.0% until the turn of the century had dwindled to less than 24.0% by

1992. The deforestation has taken place both legally and illegally. Thus it is highly important to analyse the Land degradation in Sri Lanka.

As the increasing world population places more demands on land for food production etc., many marginal arid and semiarid lands will be at risk of degradation. The need to maintain sustainable use of these lands requires that they be monitored for the onset of land degradation so that the problem may be addressed in its early stages. Monitoring will also be required to assess the effectiveness of measures to control land degradation.

1.3. Objectives

The goal of this study is to demonstrate the integrated use of remote sensing and GIS in addressing land degradation risk and severity of the Hambantota district in Sri Lanka. Generating NDVI, NDSDI, NDBI and NDWI index maps are the secondary objectives of this study.

1.4. Scope and Limitations

The study area was limited around the Hambantota district. It was assumed that this area is more suitable than other areas in the country for the analysis because the area is highly urbanized due to the recent development. Due to time limitation and also clouds on satellite images, research was focused only for two data sets (2005 and 2013).Although there are many Earth observation techniques for land degradation analysis, remote sensing combined with GIS was used in this analysis.

Freely available satellite images; LANDSAT Images with low spatial resolution (30m) were used for the study. Four different indices (NDWI,NDVI,NDSDI,NDBI) were prepared for each data set and finally all indices were merge to a one index (Land degradation index), Which is represent the severity of the land degradation in district.

2. Literature Review

2.1. Use of Remote Sensing and GIS for land degradation assessment

Remote Sensing technology is evolving through time. Significant improvements have been made in terms of spectral, spatial, temporal and radiometric resolutions (Giri T., 2007). Remotely sensed image data is widely used in a range of oceanographic, terrestrial, and atmospheric applications, such as land-cover mapping, environmental modelling and monitoring, and the updating of geographical databases (Paul M. M., 2009). A geographic information system (GIS) is a computer system for capturing, storing, checking, and displaying data related to positions on Earth's surface. Thus remote sensing with GIS is a powerful and effective tool for recognizing land degradation and measure the severity of land degradation.

Many researches focused to develop the recognizing land degradation and measuring the severity of the event, after introduced remote sensing and GIS techniques than with conventional technique. Even today there are so many on-going researches regarding this interesting area. The research about a Review of Land Degradation Assessment Methods (Taimi S.K., 2008) found that the use of remote sensing in assessing and monitoring of vegetation, erosion and land degradation under different environmental conditions is quite beneficial than other methods. However, experiments which are focused to free satellite data are very important for the developing countries like Sri Lanka.

One research on Land Degradation Detection Using Geo-Information Technology for Some Sites in Iraq (Fadhil A.M., 2009) examine the use of remote sensing and GIS data for monitoring, mapping and assessing the land degradation in the upper Mesopotamian plain of Iraq. On that study five vegetative, soil and water indices related to land degradation were applied to two LANDSAT TM and ETM+ imageries to assess the extent of land degradation for the study area during the period from 1990 to 2000. The results showed a clear deterioration in vegetative cover (2,620.4 km^2), an increase of sand dune accumulations (1,018.8 km^2), and a decrease in soil/vegetation wetness (1,720.4 km^2), accounting for 12.9, 5.0, and 8.5 present, respectively, of the total study area. In addition, a decrease in the water bodies' area was detected (228.1 km^2). Sand dunes accumulations had increased in the total study area, with an annual increasing expansion rate of (10.2 $km^2 year^{-1}$) during the ten years

covered by the study. The statistical analysis of the results indicated that the soil/vegetation wetness is the biggest influence in the process of land degradation in the study area.

Another related research has been conducted in 2009. This study was covered the land degradation assessment and recommendation for a monitoring framework in Somaliland (Njeru L et al., 2009). This research was mainly focused on the declining or increasing trend of the difference between remotely sensed NDVI and rainfall-predicted NDVI over time. It was found that the land degradation is moderate to strong in Somaliland and loss of vegetation cover was identified in this study as a potential indicator for mentoring land degradation in Somaliland.

2.2. Dark object subtraction method for remove atmospheric effects

Several different atmospheric scattering or "haze" removal techniques have been developed for use with digital remotely sensed data (e.g. LANDSAT MSS and TM). Most of these techniques can be grouped into a simple dark-object subtraction method (Vincent, 1972; Chavez, 1975; Rowen et al, 1974) or more sophisticated methods that use various atmospheric transmission models, in situ field data, or require specific targets to be present in the image (Ahem et al, 1977; Otterman and Robinove, 1981).

The Dark Object Subtraction (DOS) method is an image-based technique to cancel out the haze component caused by additive scattering from remote sensing data (Chavez Jr., 1988). This method is found to be data dependent and well accepted by the geospatial community to correct light scattering in remote sensing data. So it was used in this study to remove any effect from atmosphere (haze) to have better results.

Research related to the Effectiveness of DOS (Dark-Object Subtraction) method and water index techniques to map wetlands in a rapidly urbanizing megacity with LANDSAT 8 data (Gilmore et al, 2015) had been examined the applicability of the Dark-Object Subtraction (DOS) atmospheric correction method and water-based index techniques to map wetlands in Dhaka megacity using LANDSAT 8 data. With the use of both raw data and DOS corrected imagery, the analysis revealed that DOS corrected images performed better in discriminating wetland areas. Through this research proved about the suitability of Dark Object Substation method for water-based index assessing techniques.

2.3. Change Detection

In general, change detection involves the use of multi-temporal data sets to quantitatively analyse the temporal effects of the phenomenon (Lu et al, 2004). Digital change detection aims to detect changes over time. By and large the change detection system relies on difference in radiance value between two or more dates. There is no universally optimal technique; choice depends upon the application. Change map using post classification technique of two images will only be generally as accurate as the product of the accuracies of each individual classification. Review of change detection using multi-temporal remote sensing data has been carried out (Macleod and Congation, 1998; Mas, 1999; Lu et al, 2004; Jianya, 2008).

Object-based land cover classification and change analysis in the Baltimore metropolitan area using multi-temporal high resolution remote sensing data was carried out (Zhou, 2008). The results from analyses indicated that an object based approach provides a better means for change detection than a pixel based method because it provides an effective way to incorporate spatial information and expert knowledge into the change detection process only limitation is its applicability other than high resolution data. A method for change detection in high-resolution remote sensing images by means of Multi-resolution level set (MLS) evolution and support vector machine (SVM) classification, which combined both the pixel level method and the object-level method (Cao, 2014). Radiometric normalization of image is prerequisite for any change detection (Mateos, 2010). Relative normalization based on intrinsic radiometric information of the images is an alternative method instead of absolute normalization.

There is also a different classification given by Shaoqing. Methods of change detection can be classified into three categories: characteristic analysis of spectral type, vector analysis of spectral changes and time series analysis (Shaoqing L., 2008). Characteristic analysis of spectral type is change detection based on spectral classification and calculations. The vector analysis is done by using strength and direction characteristics, and time series analysis is used to analyse process and trend of changes of monitored ground objects, based on continuously remotely sensed data (Dušan J. et at, 2015). Usually remote sensing continuous observation data conducted on the basis of gray values thus the changed region and unchanged region is determined by selecting the appropriate threshold values of gray levels in the subtraction image.

Four of the most commonly used change detection techniques were applied to detect the nature and extent of the land-cover changes in New Burg El-Arab city using LANDSAT multispectral images (Afiify, 2011). These techniques are; (1) post classification, (2) image differencing, (3) image rationing and (4) principal component analysis. Finally, a quantitative evaluation for the results of these techniques indicates better post classification comparison results. Thus the research is carryout according to the post classification method.

2.4. Change Detection by Post Classification

The aim of an image classification is to automatically categorize all pixels in an image into land cover categories (Lillesand and Kiefer, 1994). Generally speaking, images can be classified using three different methods; unsupervised, supervised, and the hybrid (a combination of the supervised and unsupervised methods) methods of classification. The method of supervised classification, is limited by accessibility to ground sampling sites, accessible areas or areas with availability of ancillary data and may be potentially expensive is field work is required (Wilkie and Finn, 1996). The research is focused to classify the images in to two categories, as an example for NDVI as Dense vegetation area and no vegetation area, the thresholds were determined by based on test and try method and then the changed area were detected by differencing the relative areas of two categories.

3. Methodology

3.1. Theoretical Background

3.1.1. LANDSAT 7 Satellite

LANDSAT 7 managed and operated by the USGS and launched on April 15, 1999, is the seventh satellite of the LANDSAT program. LANDSAT 7 was designed to last for five years, and has the capacity to collect and transmit up to 532 images per day. It is in a polar, sun-synchronous orbit with an altitude of 705 km +/- 5 km, it takes 232 orbits, or 16 days. Primary goal of LANDSAT 7 is to refresh the global archive of satellite photos and providing up-to-date and cloud-free images. The main instrument on board LANDSAT 7 is the ETM+.

The LANDSAT Enhanced Thematic Mapper Plus (ETM+) sensor is carried on LANDSAT 7, and images consist of eight spectral bands with a spatial resolution of 30 meters for Bands 1 to 7. The resolution for Band 8 (panchromatic) is 15 meters. All bands can collect one of two gain settings (high or low) for increased radiometric sensitivity and dynamic range, while Band 6 collects both high and low gain for all scenes. The approximate scene size is 170 km north-south by 183 km east-west (https://landsat.usgs.gov).

Table 3-1: Spectral bands of LANDSAT 7

	Bands	Wavelength (micrometres)	Resolution (meters)
LANDSAT 7 Enhanced Thematic Mapper Plus (ETM+)	Band 1 - Blue	0.45-0.52	30
	Band 2 - Green	0.52-0.60	30
	Band 3 - Red	0.63-0.69	30
	Band 4 - Near Infrared (NIR)	0.77-0.90	30
	Band 5 - Shortwave Infrared (SWIR) 1	1.55-1.75	30
	Band 6 - Thermal	10.40-12.50	60 * (30)
	Band 7 - Shortwave Infrared (SWIR) 2	2.09-2.35	30
	Band 8 - Panchromatic	.52-.90	15

3.1.2. LANDSAT 8 Satellite

The LANDSAT 8 program, jointly managed by NASA and the USGS launched on February 11, 2013. LANDSAT 8 provides satellite data that is in the public domain and free. The satellite orbits Earth every 99 minutes at an altitude of 705 km in a polar orbit. LANDSAT 8 collects about 400 new scenes comprising 400 GB of data every day. Processed data becomes available to the public within 24 hours of collection. OLI and TIRS are the main instruments on board LANDSAT 8.

LANDSAT 8 Operational Land Imager (OLI) and Thermal Infrared Sensor (TIRS) images consist of nine spectral bands with a spatial resolution of 30 meters for Bands 1 to 7 and 9. The ultra-blue Band 1 is useful for coastal and aerosol studies. Band 9 is useful for cirrus cloud detection. The resolution for Band 8 (panchromatic) is 15 meters. Thermal bands 10 and 11 are useful in providing more accurate surface temperatures and are collected at 100 meters. The approximate scene size is 170 km north-south by 183 km east-west (https://landsat.usgs.gov).

Table 3-2: Spectral bands of LANDSAT 8

	Bands	Wavelength (micrometres)	Resolution (meters)
LANDSAT 8 Operational Land Imager (OLI) and Thermal Infrared Sensor (TIRS)	Band 1 - Ultra Blue (coastal/aerosol)	0.43 - 0.45	30
	Band 2 - Blue	0.45 - 0.51	30
	Band 3 - Green	0.53 - 0.59	30
	Band 4 - Red	0.64 - 0.67	30
	Band 5 - Near Infrared (NIR)	0.85 - 0.88	30
	Band 6 - Shortwave Infrared (SWIR) 1	1.57 - 1.65	30
	Band 7 - Shortwave Infrared (SWIR) 2	2.11 - 2.29	30
	Band 8 - Panchromatic	0.50 - 0.68	15
	Band 9 - Cirrus	1.36 - 1.38	30
	Band 10 - Thermal Infrared (TIRS) 1	10.60 - 11.19	100 * (30)
	Band 11 - Thermal Infrared (TIRS) 2	11.50 - 12.51	100 * (30)

3.1.3. The Normalized Difference Vegetation Index (NDVI)

NDVI was first used in 1973 by Rouse et al. from the Remote Sensing Centre of Texas A&M University. Generally, healthy vegetation will absorb most of the visible light that falls on it, and reflects a large portion of the near-infrared light. Unhealthy or sparse vegetation reflects more visible light and less near-infrared light. Bare soils on the other hand reflect moderately in both the red and infrared portion of the electromagnetic spectrum (Holmeet et al, 1987).

The NDVI is calculated using Equation;

$$NDVI = \frac{(NIR - RED)}{(NIR + RED)}$$

Theoretically, NDVI values are represented as a ratio ranging in value from -1 to +1 but in practice extreme negative values represent water, values around zero represent bare soil and values over 0.6 represent dense green vegetation.

3.1.4. The Normalized Differential Sand Dune Index (NDSDI)

NDSDI was initially proposed by Ayad Mohammed Fadhil (2009). The index was based on the normalized difference between RED and SWIR2 spectral values. NDSDI applied for identify and the highlighting the existence of the sand dune accumulation of study area. This index is aimed at differentiating between sand dune accumulations, bare soils, and the other types of soils. A threshold was used in order to mask and extraction the sand dune accumulations in the processed image.

The NDSDI is calculated using Equation;

$$NDSDI = \frac{(RED - SWIR2)}{(RED + SWIR2)}$$

Value of the NDSDI range between -1 to +1, where are the sand dunes accumulations and drifting sands often take values less than zero (< 0),while the vegetative cover takes values more than zero (> 0),and the water bodies take the highest values (Fadhil A. M., 2009).

3.1.5. The Normalized Difference Water Index (NDWI)

The Normalized Difference Water Index (NDWI) was first proposed by McFeetersin (1996). It can be used to detect surface waters in wetland environments and to allow for the measurement of surface water extent (McFeeters, 1996).

The NDWI is calculated using Equation;

$$NDWI = \frac{(GREEN - NIR)}{(GREEN + NIR)}$$

NDWI ranging between -1 to +1, where NDWI greater than zero are assumed to represent water surfaces, while value less than or equal to zero are be non-water surfaces.

3.1.6. The Normalized Difference Build-up Index (NDBI)

The values of NDBI vary according to the spectral signature from medium infra-red and near infra-red band. Using the value range there can be differentiating lands with buildings and other landscape elements. It is useful in mapping the human settlements and some elements of surrounding constructions. Because of that, the NDBI index was used to analyse increments of reflectance on TM band 4 and 5 (Zha Y. et al, 2003; Xionget et al., 2012).

Here is the NDBI equation;

$$NDBI = \frac{(SWIR1 - NIR)}{(SWIR1 + NIR)}$$

NDBI values are ranging in value from -1 to +1.Negative values represent non-build up areas, positive value represent build up areas.

3.2. Study Area

Hambantota district with area extent about 2609 km^2 in Southern Province, Sri Lanka was selected as the study area. Recently huge development projects were under gone over this area such as new harbour and international airport construction etc. Because of the recent development, arid climate, water deficiency, human activities and high wind condition Hambantota area is face several challenges in ecologically. These facts stimulate to conduct study on land degradation detection using geo information technology over the Hambantota district. Figure 3-1 shows the map of study area.

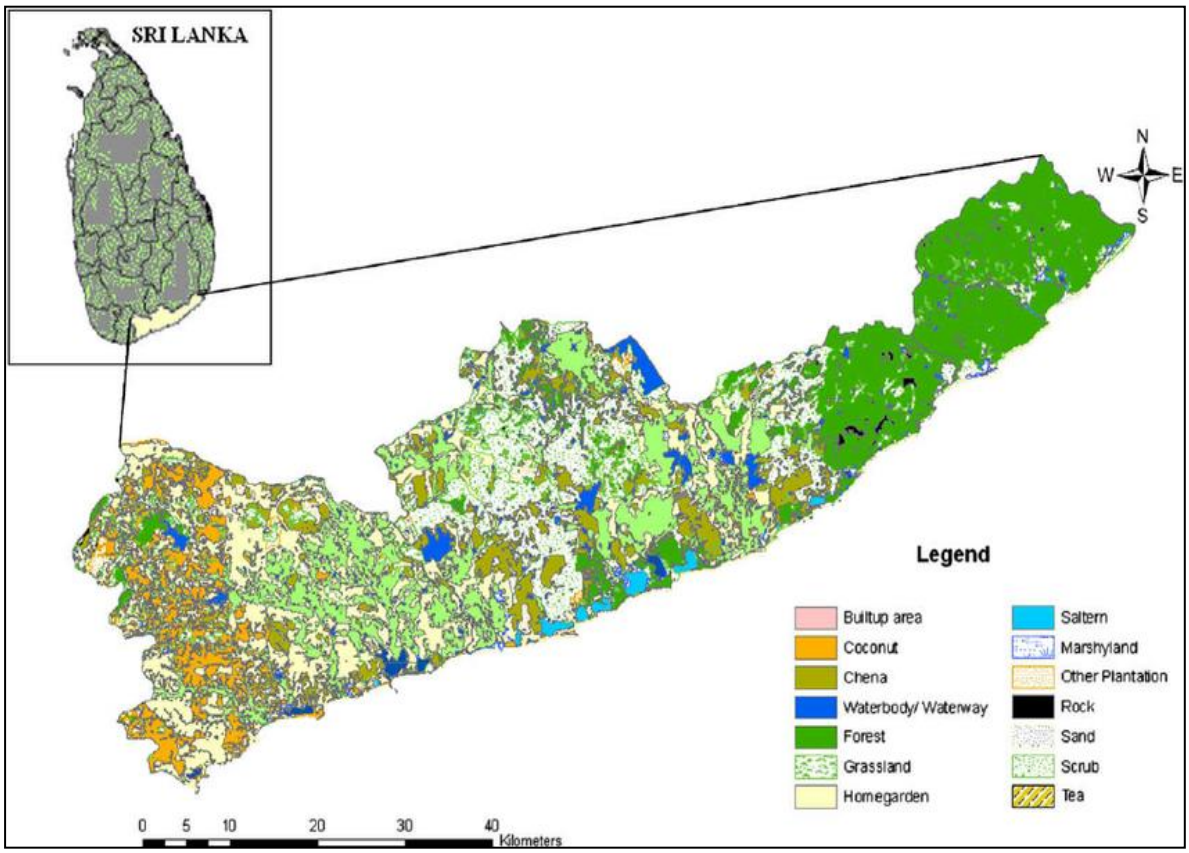

Figure 3-1: Location map of the study area

3.3. Materials used in the Research

3.3.1. Images used in the Research

LANDSAT 7 ETM+ (Enhanced Thematic Mapper Plus) and LANDSAT 8 OLI (Operational Land Imager) Level1T imagery data have been selected for this study. Level 1T product data is systematically, radiometrically, geometrically and topographically corrected; highest quality. Two satellite images were selected as pre and post images, before the recent development and after the development. All the satellite images are downloaded from Earth Explore – USGS. Characteristics of the downloaded imageries are summarized in Table 3-3.

Table 3-3: Characteristics of the downloaded imageries

Image No	Description of image	Sensor Name	Acquisition Date	Number of Bands
1	Pre Image	LANDSAT 7	2005/02/05	8
2		LANDSAT 7	2005/01/27	8
3	Post Image	LANDSAT 8	2013/07/29	11
4		LANDSAT 8	2013/08/07	11

3.3.2. Software used in the research

Below mentioned software were used for this study.

- ERDAS 9.1
- ArcGIS 10.1
- Microsoft Office Excel 2010

3.4. Schematic Diagram of the Study

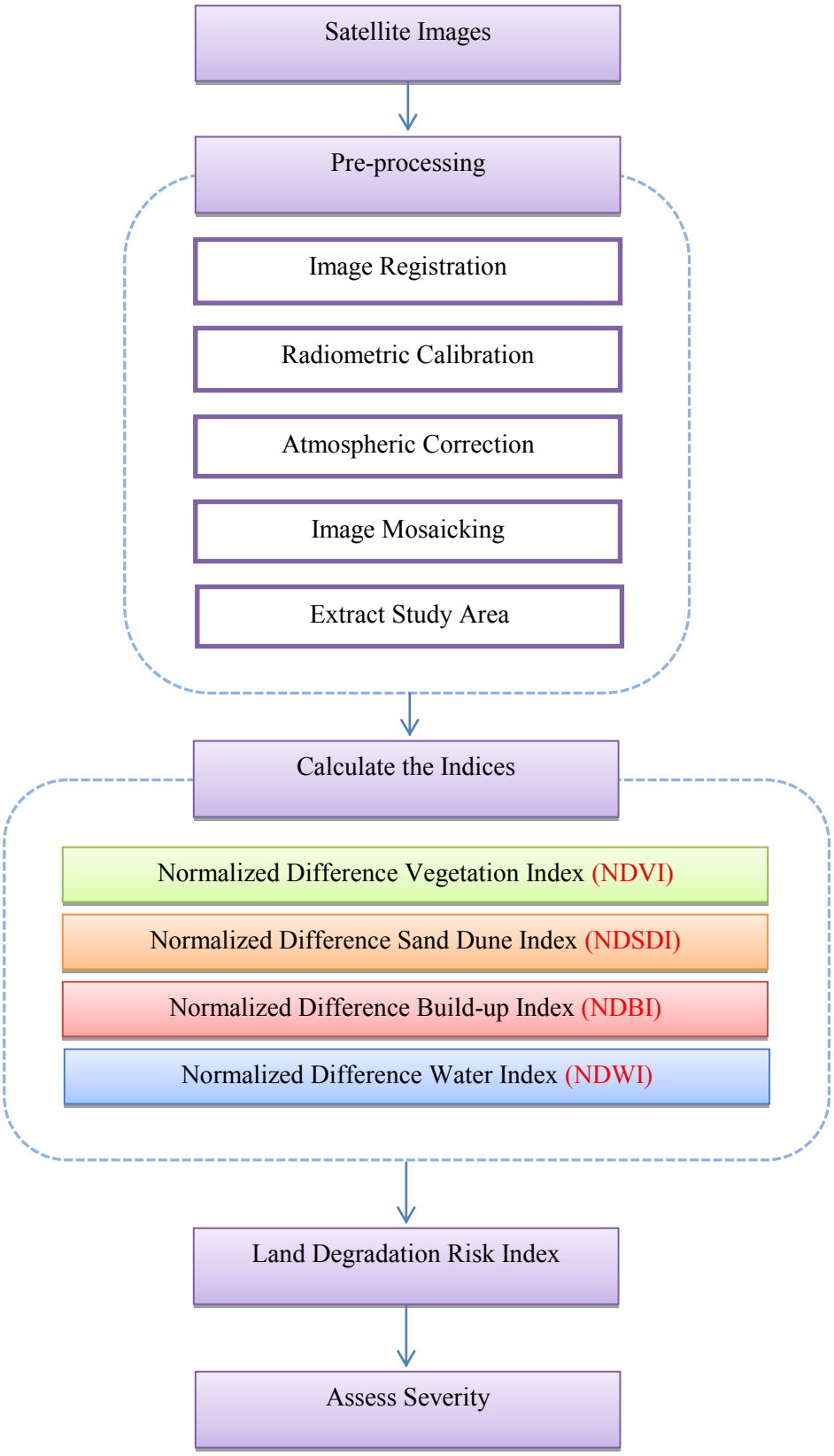

Figure 3-2: Flow Chart the methodology

Figure 3-2 describes the flow chart of the methodology followed in this study.

3.5. Image Pre-processing

After downloading the data, the imageries have been corrected for several atmospheric and sensor distortions before they used to derive indices or applying specific change detection techniques. To derive indices, both images must be equivalent geometrically and radiometrically on a pixel by pixel basis. The following procedure was carried out only for selected spectral bands (Red, SWIR1, SWIR2, Green and NIR) in order to obtain accurate spectral bands from both satellite images. The following description about image pre-processing is completely based on the relevant satellite's Hand Book which was published by USGS.

3.5.1. De-Striping LANDSAT 7 Satellite Images

On May 31, 2003, the Scan Line Corrector (SLC), which compensates for the forward motion of LANDSAT 7, failed. Without an operating SLC, the Enhanced Thematic Mapper Plus (ETM+) line of sight now traces a zigzag pattern along the satellite ground track. As a result, imaged area is duplicated, with width that increases toward the scene edge. With the SLC now permanently turned off, the ETM+ is losing approximately 22% of the data due to the increased scan gap because of this an error was found in LANDSAT 7 images. That error was on images which are taken in 2005. For accurate analysis of data those gaps should filled. For this study I used a method suggested by USGS team. This method was performed using Model Maker of ERDAS IMAGING.

For above process, it is necessary to have two images of same area from separate acquisition dates, and by using following condition filled the gaps on satellite image which was taken on 2005.

Conditional statement: **Where Image 1 > 0 uses Image 1 data, otherwise use Image 2.** Image 2 data will fill the gaps in Image 1.

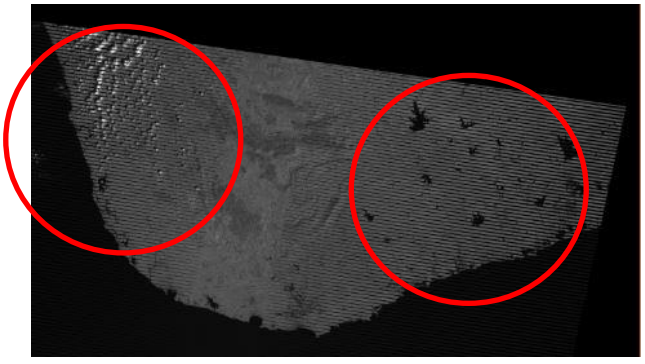

Figure 3-3: Before correcting de-stripping

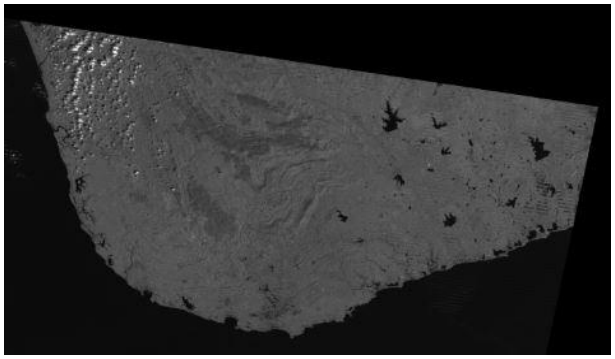

Figure 3-4: After correcting de-striping error

3.5.2. Image Registration

For this study LANDSAT images of product level 1T was used and those images are already processed to Standard Terrain Correction (Level 1T -precision and terrain correction) by the USGS. Standard Terrain Correction (Level 1T) provides systematic radiometric and geometric accuracy by incorporating ground control points while employing a Digital Elevation Model (DEM) for topographic accuracy. Geodetic accuracy of the product depends on the accuracy of the ground control points and the resolution of the DEM used: Ground control points used for Level 1T correction are derived from the GLS2000 data set. DEM sources include SRTM, NED, CDED, DTED, GTOPO 30, and GIMP. Resampling method use was Cubic Convolution with overall RMSE error around 3.7.

3.5.3. Radiometric Calibrations

Standard LANDSAT 8 and LANDSAT 7 data products provided by the USGS EROS Centre consist of quantized and calibrated scaled Digital Numbers (DN) representing multispectral image data acquired by the Enhanced thematic mapper plus (ETM+) or Operational Land Imager (OLI) and Thermal Infrared Sensor (TIRS).

The products are delivered in 16-bit unsigned integer format and can be rescaled to the Top of Atmosphere (TOA) reflectance and/or radiance using radiometric rescaling coefficients provided in the product metadata file (MTL file).

Calculation of radiance is the fundamental step in putting image data from multiple sensors and platforms into a common radiometric scale and crucial when creating multi-temporal mosaics as it largely removes variations between these images due to sensor differences, Earth-sun distance and solar zenith angle (caused by different scene dates, overpass time and latitude differences). The process involved two steps. The first step involved conversion of

measured DN to radiance using inflight sensor calibration parameters. These parameters are supplied with the imagery and are determined from comparison of inflight calibration sources with pre-flight absolute radiance values. The second step involved calculating top of atmosphere (TOA) reflectance for each band, which corrected for illumination variations (Sun angle and Earth-sun distance) within and between scenes.

3.5.4. Conversion from DN to radiance

Radiance is the amount of radiation coming from an area. To derive a radiance image from a non-calibrated image, a gain and offset must be applied to the pixel values. These gain and offset values are typically retrieved from the image's metadata file provided by the USGS. Conversion from calibrated digital numbers in L1 products back to at-sensor spectral radiance was done manually using following procedure with Model Maker in ERDAS IMAGING 2014 software. Two LANDSAT imageries (LANDSAT 7 and LANDSAT 8) were corrected by separate methods.

3.5.4.1. Equation for LANDSAT 7

$$L_\lambda = Gain * Q_{cal} + Bias$$

Where;

L_λ = the cell value as radiance

Q_{cal} = the cell value digital number

Gain = the gain value for a specific band

Bias = the bias value for a specific band

or

$$L_\lambda = \frac{(LMAX_\lambda - LMIN_\lambda)}{(QCALMAX - QCALMIN)} * (QCAL - QCALMIN) + LMIN_\lambda$$

Where;

L_λ = the cell value as radiance

QCAL = the cell value digital number

$LMIN_\lambda$ = spectral radiance scales to QCALMIN

$LMAX_\lambda$ = spectral radiance scales to QCALMAX

QCALMIN = the minimum quantized calibrated pixel value (typically = 1)

QCALMAX = the maximum quantized calibrated pixel value (typically = 255)

3.5.4.2. Equation for LANDSAT 8

$$L_\lambda = M_L Q_{cal} + A_L$$

Where;

L_λ = TOA spectral radiance

M_L = band specific multiplicative rescaling factor from the metadata

A_L = band specific additive rescaling factor from the metadata

Q_{cal} = quantized and calibrated standard product pixel values (DN)

3.5.5. Conversion radiance to reflectance and DOS1 atmospheric correction

LANDSAT 8 data are provided with band specific rescaling factors that allows for the conversion from DN to reflectance. However the effects of the atmosphere should be considered in order to measure the reflectance at the ground (Moran et al. 1992).

The surface reflectance and atmospheric correction were done by using following equations.

$$\rho = [\pi * (L_\lambda - L_P) * d^2]/[T_v * ((ESUN_\lambda * cos\theta_s * T_z) + E_{down})]$$

Where;

ρ = surface reflectance

L_λ = at satellite radiance

L_P = Path radiance

d = Earth sun distance astronomical units

T_v = Atmospheric transmittance in the viewing direction

$ESUN_\lambda$ = Mean solar exo - atmospheric irradiance

θ_s = Solar zenith angle in degrees ($\theta_s = 90 - \theta_e$, θ_e = *Sun elevation*)

T_z = Atmospheric transmittance in the illumination direction

E_{down} = Down welling diffuse irradiance

Therefore need several atmospheric equations in order to calculate rho (ρ)**.** Alternatively, it is possible to use image based techniques for the calculation of these parameters, without in situ measurements during image acquisition.

The Dark Object Subtraction (DOS) is family of image based atmospheric correction. Chavez (1996) explains that the basic assumption is that within the image some pixels are in complete shadow and their radiances received at the satellite are due to atmospheric scattering. This assumption is combined with fact that very few targets on the Earth's surface are absolute black, so an assumed one percent minimum reflectance is better than zero percent. It is worth

point out that the accuracy of image based techniques is generally lower than physically based corrections, but they are very useful when no atmospheric measurements are available as they can improve the estimation of land surface reflectance. The path radiance is given by (Sobrino et al, 2004).

$$L_P = L_{min} - L_{DO1\%}$$

Where;

L_p = Path radiance

L_{min} = Radiance that corresponds to a digital count value for which the sum of all the pixels with digital counts lower or equal to this value is equal to the 0.01% of all the pixels from the image considered" (Sobrino et al., 2004, p. 437), therefore the radiance obtained with that digital count value (DN_{min})

$L_{DO1\%}$ = Radiance of Dark Object, assumed to have a reflectance value of 0.01

Therefore;

$$L_{min} = M_L * DN_{min} + A_L$$

The radiance of Dark Object is given by;

$$L_{DO1\%} = 0.01 * [(ESUN_\lambda * cos\theta_s * T_z) + E_{down}] * T_v/(\pi * d^2)$$

Therefore path radiance;

$$L_P = M_L * DN_{min} + A_L - 0.01 * [(ESUN_\lambda * cos\theta_s * T_z) + E_{down}] * T_v/(\pi * d^2)$$

There are several DOS techniques (e.g. DOS1, DOS2, DOS3, DOS4) based on different assumption about T_v, T_z and E_{down}. The simplest technique is the DOS1, where the following assumptions are made (Moran et al, 1992).

$T_v = 1$, $T_z = 1$, $E_{down} = 0$

Therefore the path radiance;

$$L_P = M_L * DN_{min} + A_L - 0.01 * (ESUN_\lambda * cos\theta_s)/(\pi * d^2)$$

Finally surface reflectance given by;

$$\rho = [\pi * (L_\lambda - L_P) * d^2]/(ESUN_\lambda * cos\theta_s)$$

$ESUN_\lambda$ value can be calculated by using following equation.

$$ESUN_\lambda = (\pi * d^2) * RADIANCE\_MAXIMUM/REFLECTANCE\_MAXIMUM$$

Where, RADIANCE_MAXIMUM and REFLECTANCE_MAXIMUM are provided by image data file.

3.5.6. Mosaicking and Extracting the Study area

After correcting the selected bands for distortions, not only the bands of image no 1 and 2 but also the bands of image 3 and 4 were mosaicked with each other by using ERDAS imaging, because the study area was fallen on both images partially. Then study area was extracted by respective bands of both satellite images using Arc Map 10.1. Mosaicked and extracted images were shown on Figure 3-5.

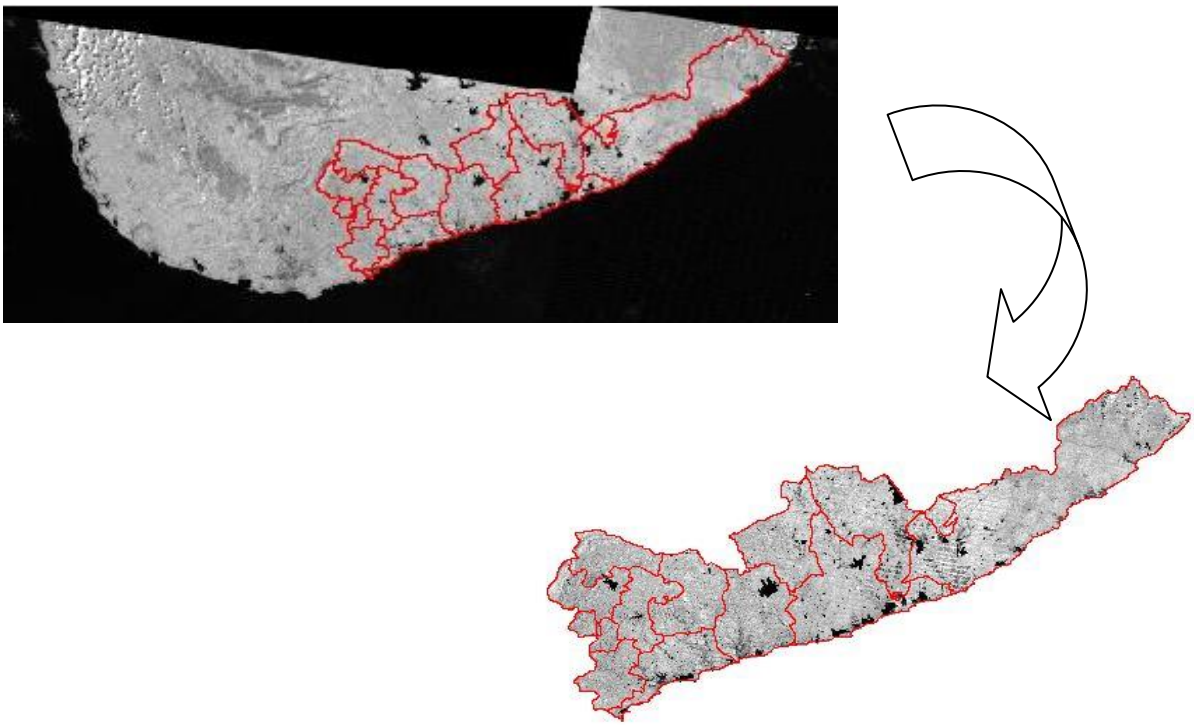

Figure 3-5: Extract the study area from mosaic image

3.6. Indices calculation

The research was based on four different indices namely NDWI, NDVI, NDBI and NDSDI. These indices were derived for both pre and post images by using ERDAS IMAGING Model Maker. The models which were prepared in order to derive the indices were represented in below sections. Regarding this indices a well-focused description is mentioned under chapter 3.

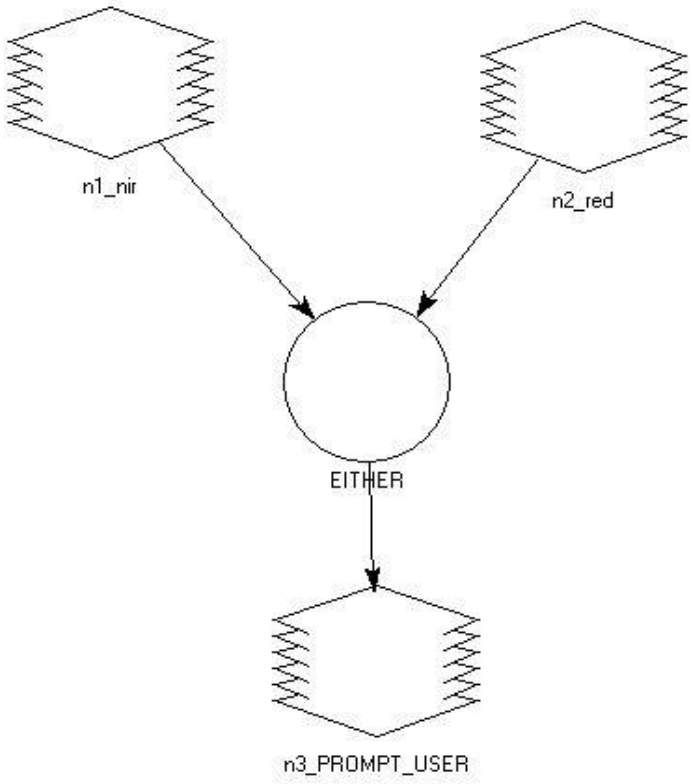

Figure 3-6: Model of the NDVI calculation

Ignorance zero value is most important part of the NDVI calculation. If it is not zero value of the pixel may be damage the result. Following equation was used to do the ignorance of zero for model.

EITHER 0 IF {($n1_nir + $n2_red) = 0} OR {($n1_nir - $n2_red) / ($n1_nir + $n2_red)} OTHERWISE

Same procedure was used for other three indices; NDSDI, NDBI and NDWI.

3.7. Threshold determination for post classification

After generating the indices map, a threshold value was determined for every index to classify the map in to two classes. As an example the threshold value for the NDVI was used to find the dense vegetation areas and less vegetation areas.

Selected threshold values were tabulated on table 3-4 and the selection was completely based on trial and test method and the visual interpretation. Calculating threshold via ground field observation is more time consuming and expensive so trial and test method was done.

Table 3-4: Threshold values for indices

Index	Class name	Threshold Value
NDVI	Less vegetation	-1 to 0.3
	Dense vegetation	0.3 to 1
NDSDI	Sand accumulated area	-1 to 0
	Other area	0 to 1
NDBI	Non-build-up area	-1 to 0.3
	Build-up area	0.3 to 1
NDWI	Land area	-1 to 0
	Water bodies	0 to 1

3.8. Land degradation index

Land degradation Index (LDI) is indicative of the overall degree of the difficulty in rehabilitating degraded land in a given region for productive use (Fadhil A.M., 2009). The vegetative cover and the sand dunes accumulation and build-up area in Hambantota were used for this assessment which derived from both LANDSAT 7 and 8 imageries using NDVI, NDSDI and NDBI algorithms, respectively. The higher value of LDI indicates a more severe level of land degradation. Land Degradation Index (LDI) is calculated using the following formula.

$$Land\ Degradation\ Index\ (LDI)\ = \sum_{i=1}^{n} PC_i^{-q}$$

Where;

LDI = the risk of the land degradation in the area ($0 \leq LDI \leq 1$)

C_i = the rank at which the land in an assessment unit has been degraded

P = the areal percentage of the land having a rank I

n = the number of indicator classes (three in this case)

q = the exponent of rank

Three indicators have been identified as critical to assessment the desertification severity in the study area: vegetation cover, extent of drifting sand, build-up area. The first two factors are prime indicators of the land degradation. All indicators are directly derived from satellite imagery. The increase of build-up area is one of significant factor that influencing strongly and leading to accelerated land degradation by creating a great pressure on the land and other natural resources. The threshold for each rank of a given indicator was set in accordance with the United Nations' indices for desertification assessment (UNEP, 1992).

Table 3-5: Indices and weights for factors used in the assessment of land degradation risk in the study area

Indicator	**Severity Level**				**Weight**
	I Severe	**II High**	**III Medium**	**IV Low**	
Vegetation cover (%)	<10	10-25	25-40	>40	0.40
Drifting sand coverage (%)	>65	15-65	5-15	<5	0.25
Build up area (%)	>35	15-35	5-15	<5	0.35

The values 0.40, 0.25, and 0.35 were selected as weights for each and every indicator by experimentation in this study for vegetation cover, drifting sand coverage build up area respectively. The method for this selection was Trial and error method which is a fundamental method of problem solving. It is characterized by repeated, varied attempts which are continued until success or until the agent stops trying.

4. Results and Discussion

After pre-processing the images, NDVI, NDSDI, NDBI, NDWI and LDI indices were calculated by using LANDSAT 7 ETM+ and LANDSAT 8 OLI imageries. Then it was tried to analyse the environmental changes and assess the land degradation severity of study area.

4.1. NDVI (Normalized difference vegetation index) Estimation

The results obtained for NDVI estimated images were classified into two classes as less vegetation and dense vegetation. The resultant NDVI maps for year 2005 and 2013 are shown in figure 4-1 and figure 4-2 respectively.

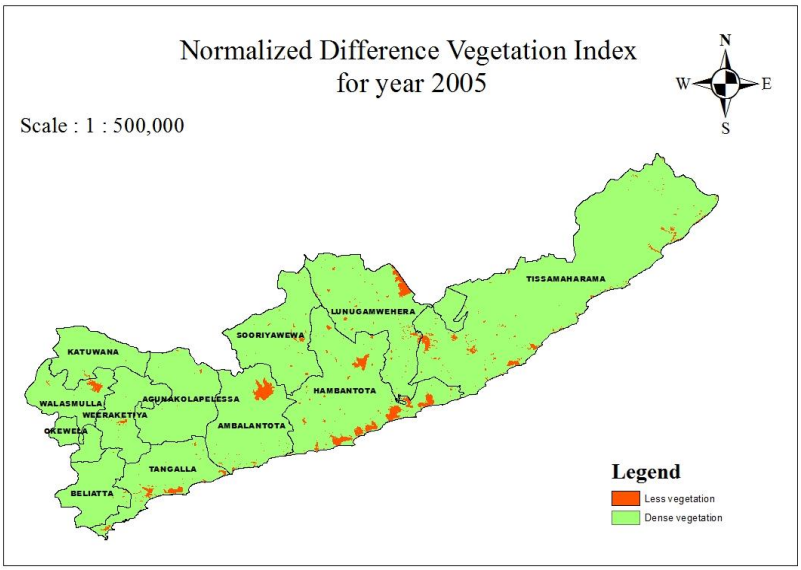

Figure 4-1: NDVI for Landsat7 ETM+ image in 2005

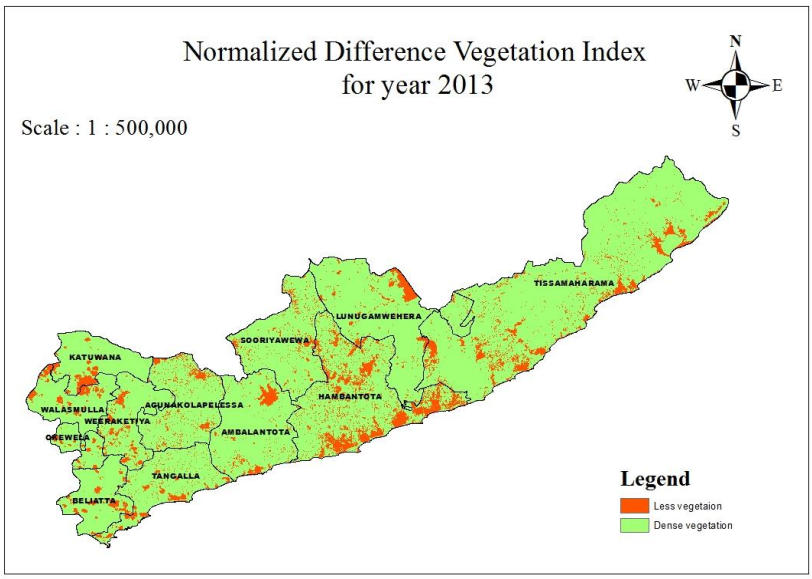

Figure 4-2: NDVI for Landsat8 OLI image of 2013

Those figures exhibits that decreasing of the vegetated land from the year 2005 to year 2013.Then the classified maps were used to calculate the extent of the vegetation cover in both years. Table 4-1 shows the extent of the vegetation cover in both years with respect to the divisional secretariat boundaries.

Table 4-1: Divisional secretarial area vegetation cover extracted by NDVI results of the study area for the period of 2005 to 2013

Divisional secretariat area name	Total area	2005		2013		2013 - 2005		Vegetation change rate
	km^2	km^2	%	km^2	%	km^2	%	km^2Year^{-1}
Agunakolapelessa	172.333	171.924	99.763	153.510	89.078	-18.414	-10.685	-2.302
Ambalantota	213.442	203.655	95.414	194.504	91.127	-9.151	-4.287	-1.144
Beliatta	105.300	98.459	93.503	94.465	89.710	-3.994	-3.793	-0.499
Hambantota	351.371	325.159	92.540	262.439	74.690	-62.720	-17.850	-7.840
Katuwana	108.936	108.577	99.670	97.185	89.213	-11.392	-10.458	-1.424
Lunugamwehera	291.438	280.490	96.243	267.703	91.856	-12.786	-4.387	-1.598
Okewela	44.715	44.695	99.956	40.226	89.960	-4.469	-9.995	-0.559
Sooriyawewa	193.332	190.917	98.751	177.735	91.933	-13.182	-6.818	-1.648
Tangalle	150.260	142.497	94.833	133.133	88.601	-9.364	-6.232	-1.171
Tissamaharama	777.537	760.751	97.841	703.876	90.526	-56.876	-7.315	-7.109
Walasmulla	103.616	100.537	97.029	91.439	88.248	-9.098	-8.781	-1.137
Weeraketiya	114.224	113.334	99.222	99.949	87.503	-13.386	-11.719	-1.673
Sum	2626.503	2540.995	96.744	2316.162	88.184	-224.834	-8.560	-28.104
Average								-3.513

From the table 4-1 it can be seen that the total vegetation cover has decreased from 96.744% to 88.184% during the period of eight years. The vegetation cover changing rate is -3.513km^2Year^{-1} for the study area and it shows a significant decrease in vegetation cover. In the comparison of the vegetative cover of the area for each Divisional secretariat area during the two years 2005 and 2013, it was observed a decrease in the vegetative cover in all of the studied regions. According to the table 4-1 it is clear that within Hambantota, Weeraketiya, Katuwana and Agunakolapelessa divisional secretariat areas registered the worst situation and

the highest decline in the vegetative cover during the mentioned years. They were 17.85%, 11.719%, 10.685% and 10.458% of the total area of each region, respectively.

4.2. NDBI (Normalized difference building index) Estimation

NDBI index shows the build-up area in the study area for both years. After calculating the NDBI index, the resulted maps were classified into two categories as build-up area and non-build-up area. Figure 4-3 and figure 4-4 displays the created NDBI maps for the study area in year 2005 and year 2013 respectively.

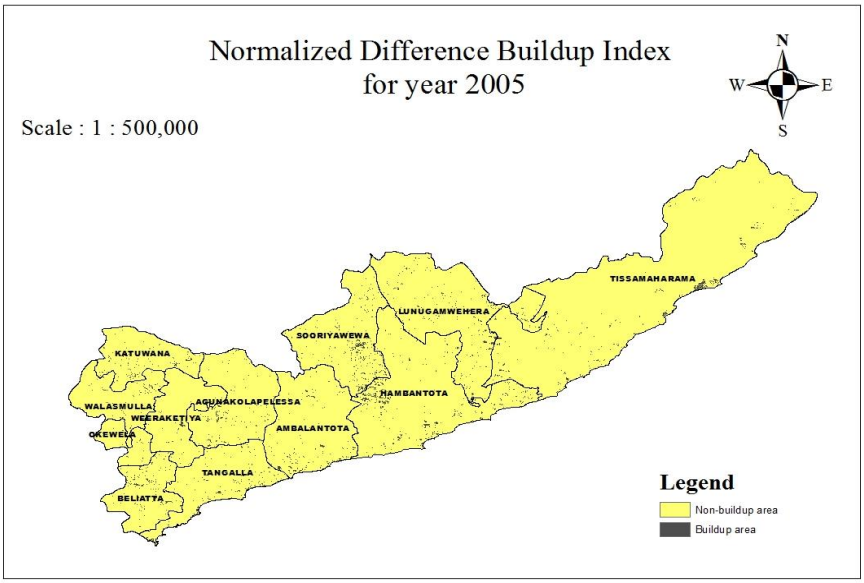

Figure 4-3: Classified NDBI map for year 2005

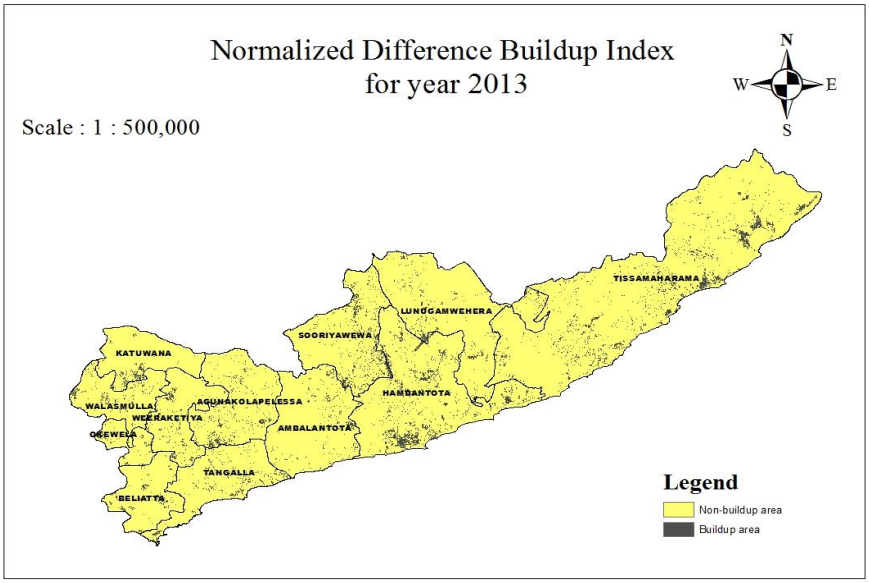

Figure 4-4: Classified NDBI map for year 2013

These classified maps were then used to extract the build-up area. The result shows that built up area in 2005 were 48.335 km^2 which has increased to 132.068 km^2 by the year 2013 i.e. an increase of 83.732 km^2 in 8 years period.

Table 4-2: Build-up area of divisional secretarial area, extracted by NDBI results of the study area for the period of 2005 to 2013

Divisional secretariat area name	Total area	2005		2013		2013-2005		Build-up area change rate
	km2	km2	%	km2	%	km2	%	km^2Year^{-1}
Agunakolapelessa	172.333	3.148	1.827	9.380	5.443	6.232	3.616	0.779
Ambalantota	213.442	3.990	1.869	6.738	3.157	2.749	1.288	0.344
Beliatta	105.300	3.011	2.860	4.803	4.562	1.792	1.702	0.224
Hambantota	351.371	9.394	2.674	28.128	8.005	18.734	5.332	2.342
Katuwana	108.936	2.357	2.164	4.214	3.868	1.857	1.704	0.232
Lunugamwehera	291.438	5.331	1.829	9.898	3.396	4.568	1.567	0.571
Okewela	44.715	0.727	1.626	1.975	4.416	1.247	2.790	0.156
Sooriyawewa	193.332	5.778	2.989	14.140	7.314	8.362	4.325	1.045
Tangalle	150.260	3.791	2.523	7.106	4.729	3.315	2.206	0.414
Tissamaharama	777.537	8.148	1.048	35.869	4.613	27.721	3.565	3.465
Walasmulla	103.616	1.446	1.396	4.261	4.112	2.814	2.716	0.352
Weeraketiya	114.224	1.214	1.063	5.558	4.865	4.343	3.803	0.543
Sum	2626.503	48.335	1.840	132.068	5.028	83.732	3.188	10.467
Average								1.308

By observing table 4-2 it can be said that land degradation increasing from the low degraded (IV) level to medium level (III). The rate of change of build-up area for the study area is 1.308km^2Year^{-1}.

4.3. NDSDI (Normalized difference sand dune index) Estimation

By applying the Equation 02, NDSDI values for both satellite images were calculated, and based on these values; the area was classified into two classes as sand accumulated areas and other areas. The resulted maps are shown in figure 4-5 and figure 4-6.

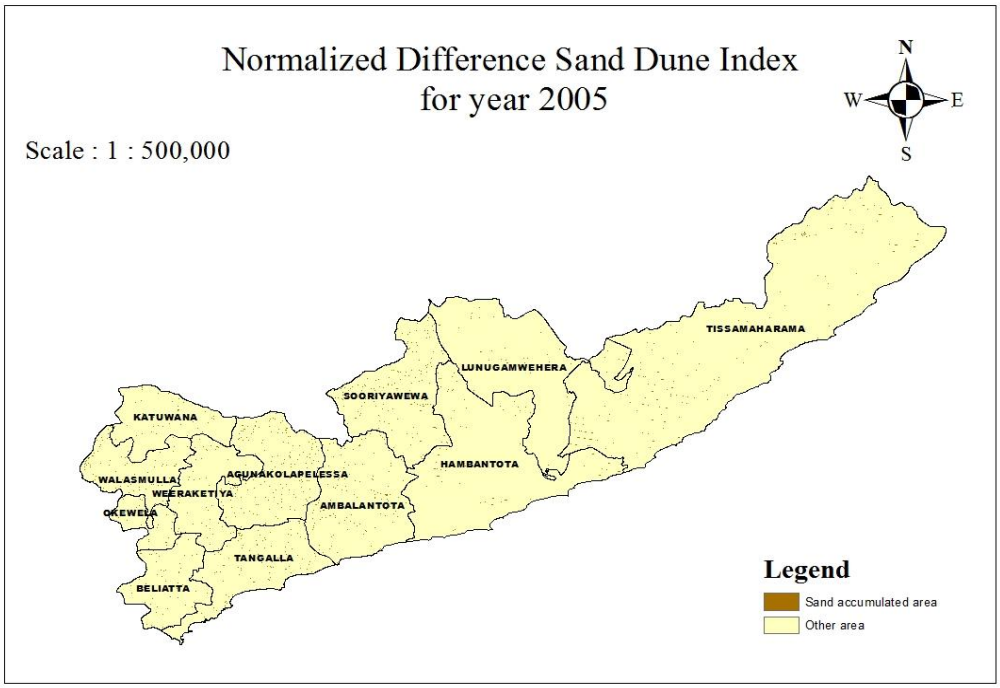

Figure 4-5: Classified NDSDI for Hambantota area in 2005

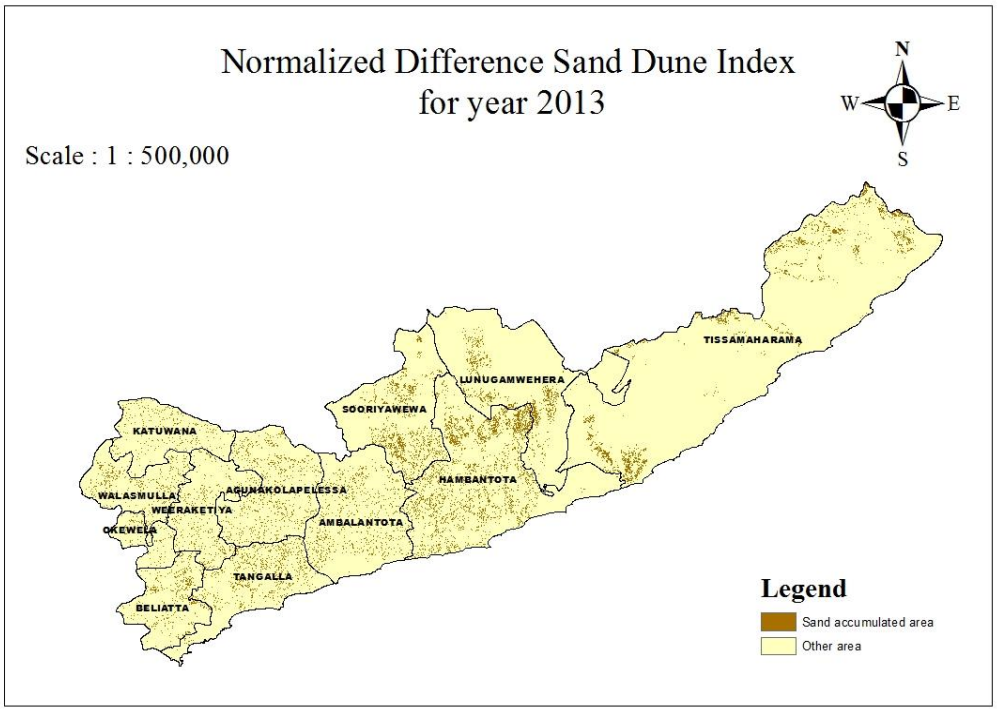

Figure 4-6: Classified NDSDI for Hambantota in 2013

As same as the above two methods the area extents responsible for the sand dune accumulation were calculated for both NDSDI indices maps by using Raster calculator in ArcGIS 10.1. Then it was found the difference of the accumulated sand extent for the area in past 8 years. The results are tabulated in the table 4-3.

Table 4-3: Sand dune accumulation of divisional secretarial area, extracted by NDSDI results of the study area for the period of 2005 to 2013

Divisional secretariat area name	Total area	2005		2013		2013-2005		Sand accumulation change rate
	km^2	km^2	%	km^2	%	km^2	%	km^2Year^{-1}
Agunakolapelessa	172.333	2.804	1.627	13.066	7.582	10.262	5.955	1.283
Ambalantota	213.442	2.471	1.158	12.814	6.004	10.343	4.846	1.293
Beliatta	105.300	0.916	0.870	6.587	6.256	5.671	5.385	0.709
Hambantota	351.371	1.358	0.387	40.266	11.460	38.908	11.073	4.863
Katuwana	108.936	0.869	0.798	5.319	4.883	4.450	4.085	0.556
Lunugamwehera	291.438	0.886	0.304	11.913	4.088	11.028	3.784	1.378
Okewela	44.715	0.559	1.250	2.344	5.241	1.785	3.991	0.223
Sooriyawewa	193.332	2.715	1.404	15.631	8.085	12.916	6.681	1.614
Tangalle	150.260	2.031	1.352	12.337	8.211	10.306	6.859	1.288
Tissamaharama	777.537	3.445	0.443	27.217	3.500	23.772	3.057	2.971
Walasmulla	103.616	1.535	1.482	6.715	6.481	5.180	4.999	0.647
Weeraketiya	114.224	1.007	0.882	7.604	6.657	6.597	5.776	0.825
Sum	2626.503	20.598	0.784	161.814	6.161	141.215	5.377	17.652
Average								2.206

By observing the above table it can be noted that the sand dune accumulation of the study area has a variation from 0.784% to 6.161%. The rate of change of sand dune accumulation is 34290km^2Year^{-1}. It was increased from low level (IV) to medium level (III).

4.4. NDWI (Normalized difference water index) Estimation

NDWI index was computed for the multi-temporal Landsat ETM+ and OLI images in order to obtain the water bodies in the study area. The results were shown in figure 4-7 and figure 4-8.

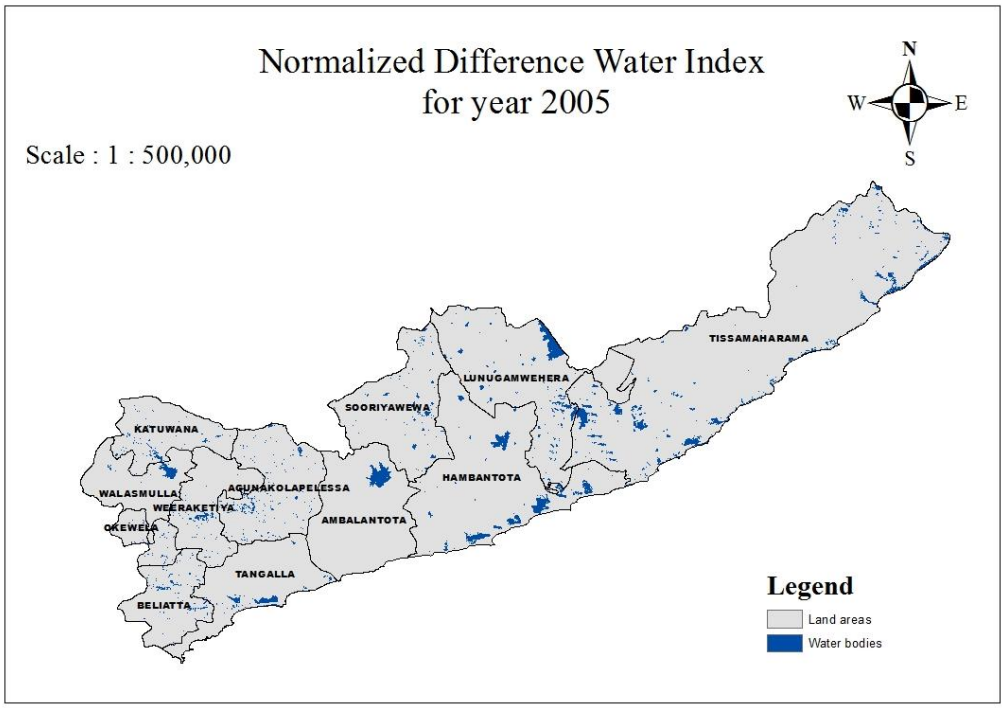

Figure 4-7: Normalized difference water index for year 2005

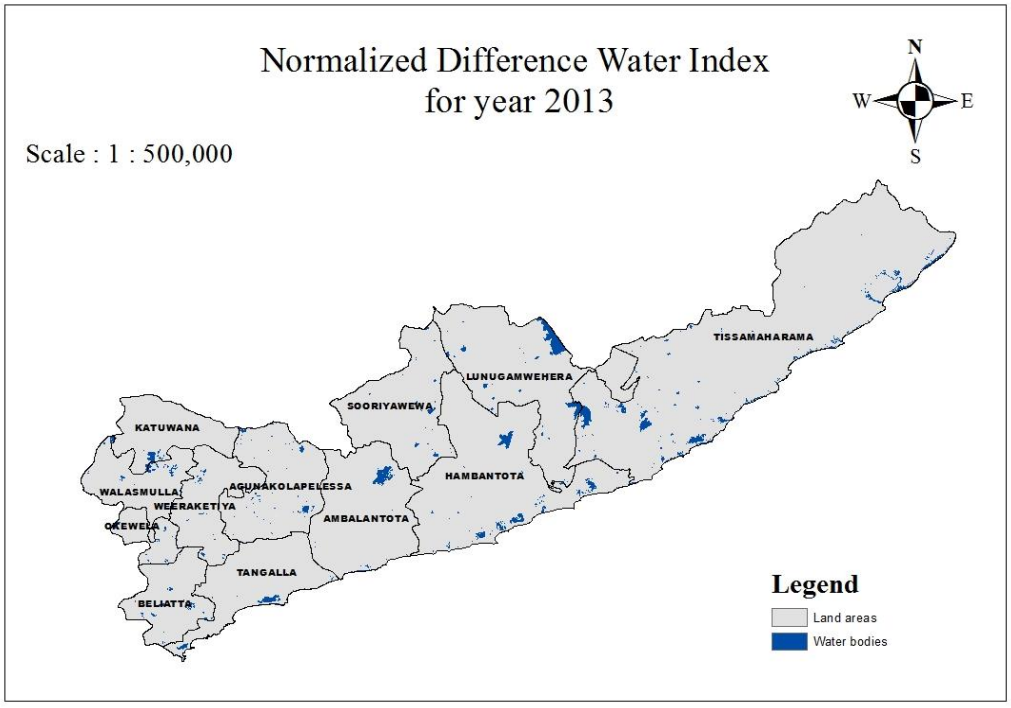

Figure 4-8: Normalized difference water index for year 2013

Results of NDWI clarified a significant decrease in the area covered by water bodies during the study period from 2005 to 2013.The calculated water content of the area and decrement of the water content within these 8 years is tabulated in table 4.4 for both 2005 and 2013.

Table 4-4: Water content of divisional secretarial area, extracted by NDWI results of the study area for the period of 2005 to 2103

Divisional secretariat area name	Total area	2005		2013		2013-2005		Water bodies decrease rate
	km^2	km^2	%	km^2	%	km^2	%	km^2Year^{-1}
Agunakolapelessa	172.333	5.4378	3.155	3.236	1.878	2.201	1.277	0.275
Ambalantota	213.442	6.3531	2.976	4.392	2.058	1.961	0.919	0.245
Beliatta	105.300	3.0501	2.897	1.986	1.886	1.064	1.010	0.133
Hambantota	351.371	16.6617	4.742	8.959	2.550	7.703	2.192	0.963
Katuwana	108.936	3.1266	2.870	1.806	1.658	1.320	1.212	0.165
Lunugamwehera	291.438	13.3209	4.571	10.975	3.766	2.346	0.805	0.293
Okewela	44.715	1.4067	3.146	1.035	2.315	0.372	0.831	0.046
Sooriyawewa	193.332	3.1707	1.640	1.986	1.027	1.184	0.613	0.148
Tangalle	150.260	4.5162	3.006	3.169	2.109	1.347	0.897	0.168
Tissamaharama	777.537	28.0071	3.602	18.660	2.400	9.347	1.202	1.168
Walasmulla	103.616	3.1689	3.058	2.498	2.410	0.671	0.648	0.084
Weeraketiya	114.224	2.3499	2.057	1.229	1.076	1.121	0.981	0.140
Sum	2626.503	90.570	3.448	59.931	2.282	30.639	-1.167	3.830
Average								0.479

4.5. Assessment of Land Degradation Severity

NDVI, NDSDI and NDBI indices maps derived for the year 2005 and 2013 data sets, showed a decrease in the vegetation cover and an increase in the sand dune accumulation and the build-up area of the study area. Land degradation severity of the area was calculated by using above three indices (Related procedure was mentioned on chapter 3.8) and found the severity level for all divisional secretarial areas. Finally estimated NDWI index was used to represent the effect of the degradation on the area.

4.5.1. Calculated LDI for year 2005

Table 4-5: Calculated Land degradation index for year 2005

Divisional Secretariat Area	Non vegetation Cover (q=0.4)		Drifting Sand Coverage (q=0.25)		Build-up area (q=0.35)		LDI 2005
	P	C i	P	C i	P	C i	
Agunakolapelessa	0.237	4.00	1.627	4.00	1.827	4.00	0.024
Ambalantota	4.586	4.00	1.158	4.00	1.869	4.00	0.046
Beliatta	6.497	4.00	0.870	4.00	2.860	4.00	0.061
Hambantota	7.460	4.00	0.387	4.00	2.674	4.00	0.062
Katuwana	0.330	4.00	0.798	4.00	2.164	4.00	0.021
Lunugamwehera	3.757	4.00	0.304	4.00	1.829	4.00	0.035
Okewela	0.044	4.00	1.250	4.00	1.626	4.00	0.019
Sooriyawewa	1.249	4.00	1.404	4.00	2.989	4.00	0.036
Tangalle	5.167	4.00	1.352	4.00	2.523	4.00	0.055
Tissamaharama	2.159	4.00	0.443	4.00	1.048	4.00	0.022
Walasmulla	2.971	4.00	1.482	4.00	1.396	4.00	0.036
Weeraketiya	0.778	4.00	0.882	4.00	1.063	4.00	0.017

Land degradation index for each divisional secretariat area in year 2005 was very small in value because during this period there was a minor development in the area.

4.5.2. Calculated LDI for 2013

Table 4-6: Calculated Land degradation index for year 2013

Divisional Secretariat Area	Non vegetation Cover (q=0.4)		Drifting Sand Coverage (q=0.25)		Build-up area (q=0.35)		LDI 2013
	P	C i	P	C i	P	C i	
Agunakolapelessa	10.922	4.00	0.449	3.000	5.443	2.000	0.109
Ambalantota	8.873	4.00	0.439	3.000	3.157	4.000	0.074
Beliatta	10.290	4.00	0.446	3.000	4.562	4.000	0.091
Hambantota	25.310	4.00	0.536	3.000	8.005	3.000	0.204
Katuwana	10.787	4.00	0.448	4.000	3.868	4.000	0.089
Lunugamwehera	8.144	4.00	0.435	4.000	3.396	4.000	0.071
Okewela	10.040	4.00	0.445	3.000	4.416	4.000	0.088
Sooriyawewa	8.067	4.00	0.435	3.000	7.314	3.000	0.099
Tangalle	11.399	4.00	0.451	3.000	4.729	3.000	0.101
Tissamaharama	9.474	4.00	0.442	4.000	4.613	3.000	0.089
Walasmulla	11.752	4.00	0.453	3.000	4.112	4.000	0.096
Weeraketiya	12.497	4.00	0.457	3.000	4.865	4.000	0.105

Table 4-5 and 4-6 highlighted that almost in all divisional secretariat areas Land Degradation Index increase from year 2005 to year 2013. For easy comparison, two Land degradation indices are represented as a graph shown in figure 4-9. This graph shows that there is an expansion in degradation in the area.

4.5.3. Graph for Land Degradation Index in study area

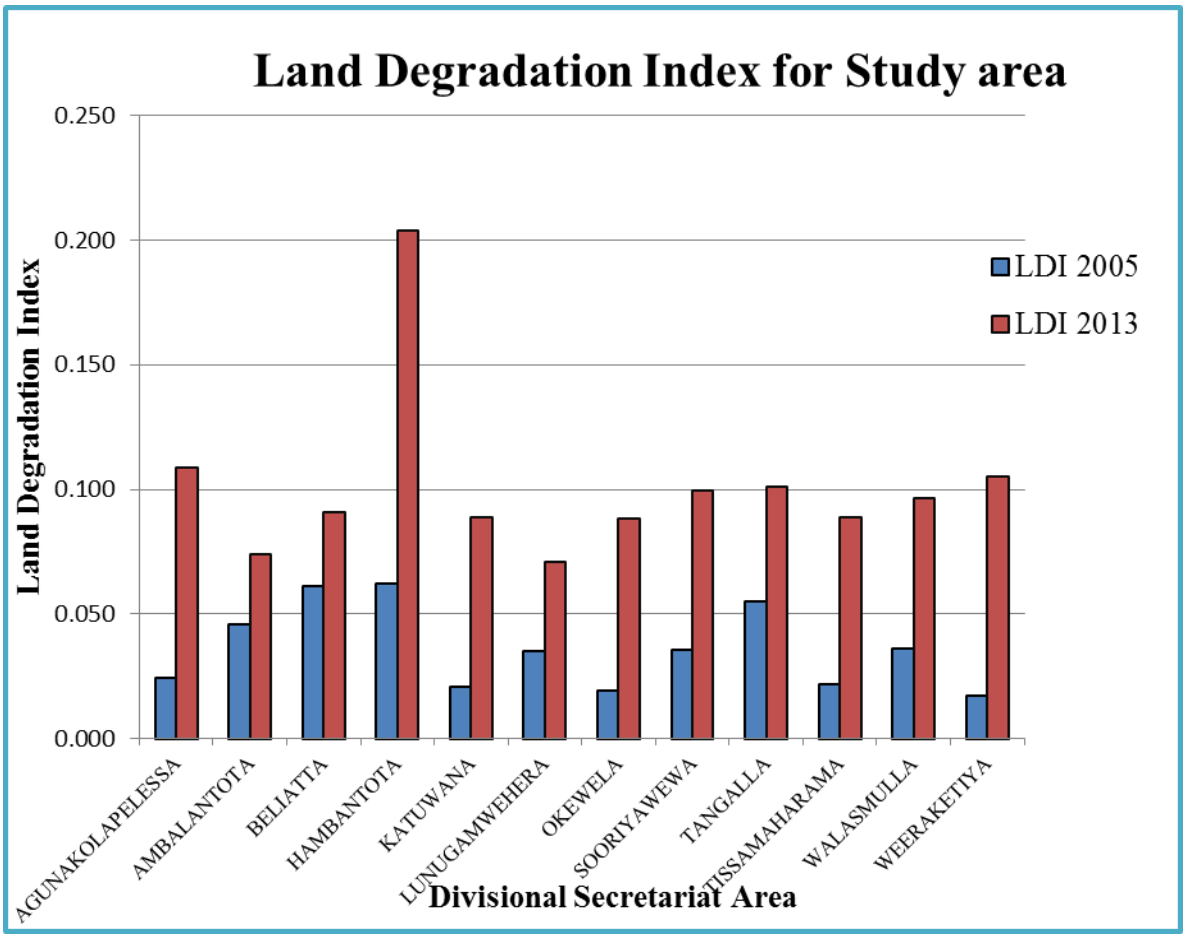

Figure 4-9: Land degradation index in Hambantota district for year 2005 and 2013

According to the above mentioned results Hambantota town has highest magnitude of severity and it was increased by 0.142 in past 8 years. This occurs mainly due to the recent development of the area.

After finding the LDI for each divisional secretariat area, the next task was to find the overall LDI for Hambantota district.

The Table 4-7 shows the LDI in overall Hambantota district for above mentioned years.

Table 4-7: Land degradation index for Hambantota district

District	Year	Non vegetation Cover (q=0.4)		Drifting Sand Coverage (q=0.25)		Build-up area (q=0.35)		LDI
		P	C i	P	C i	P	C i	
Hambantota	2005	3.256	4.000	0.784	3.000	1.84	2.000	0.035571
	2013	11.816	4.000	6.161	3.000	5.028	4.000	0.154127

Figure 4-10 shows a graphical representation of LDI in 2005 and 2013.

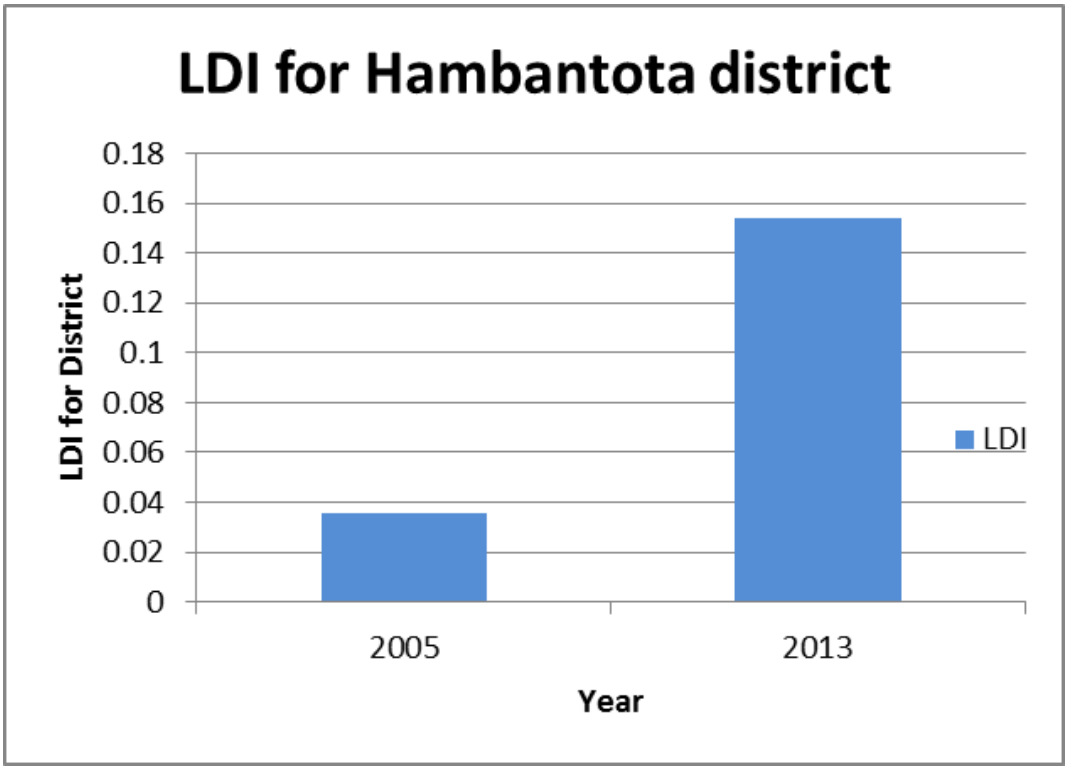

Figure 4-10: Land degradation index for Hambantota district

4.6. The relationship between Land degradation rate and water decreasing rate

A research related on Land Degradation Detection Using Geo- Information Technology for Some Sites in Iraq (Fadil A.M., 2009) has obtained the deficiency of water as the most effective factor on the land degradation acceleration in the study area, in addition to the socio-economic factors. Thus, land degradation rate and water decreasing rate in the study area were analysed in order to find the correlation between them.

Table 4-8 and figure 4-11 represent the calculated Land degradation rate in study area for considered 8 years.

Table 4-8: Land degradation rate for divisional secretariat area

Divisional Secretariat Area	Land degradation Rate
Agunakolapelessa	8.47334122
Ambalantota	2.7699734
Beliatta	2.94967683
Hambantota	14.1897793
Katuwana	6.80826285
Lunugamwehera	3.57764206
Okewela	6.91210995
Sooriyawewa	6.3930561
Tangalle	4.63287361
Tissamaharama	6.69586141
Walasmulla	6.01167476
Weeraketiya	8.7953548

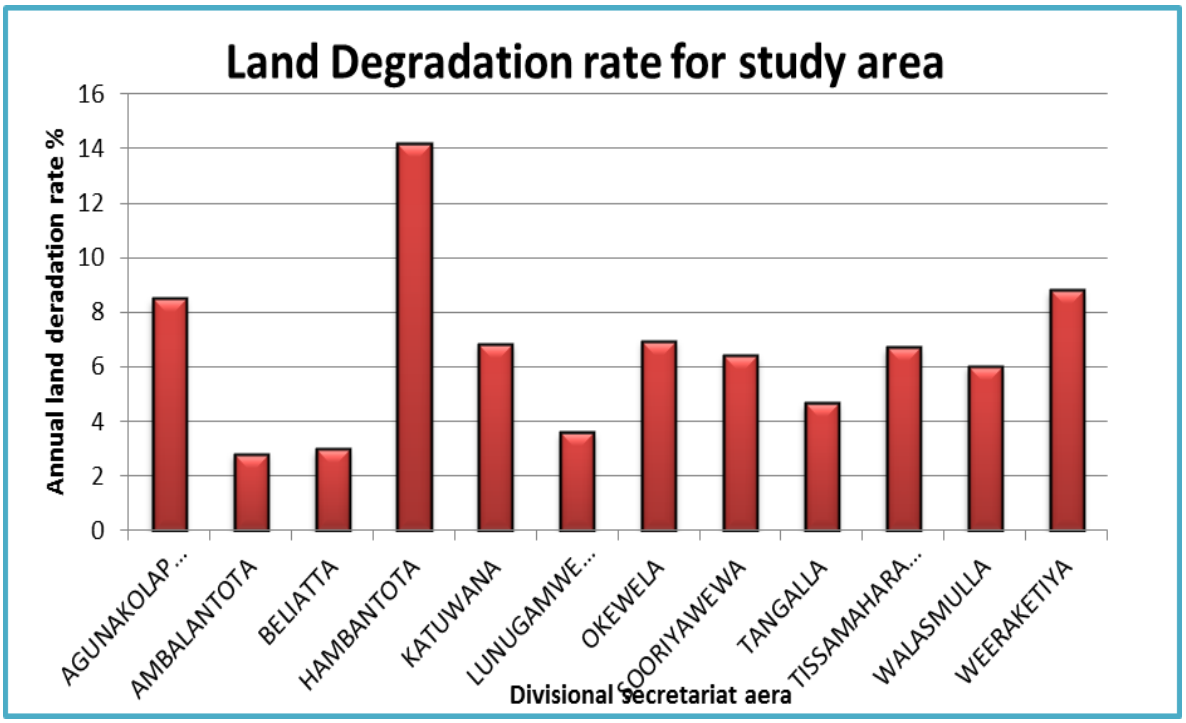

Figure 4-11: Land degradation rate for study area

Table 4-9 and figure 4-12 represent the calculated water decreasing rate in study area for considered 8 years.

Table 4-9: Water decreasing rate

Divisional secretariat area name	Water decreasing rate
Agunakolapelessa	1.577411
Ambalantota	0.918797
Beliatta	1.010256
Hambantota	3.192299
Katuwana	1.211996
Lunugamwehera	0.805077
Okewela	0.83127
Sooriyawewa	0.612626
Tangalle	0.896643
Tissamaharama	1.402181
Walasmulla	0.647969
Weeraketiya	2.980972

When considering the increment percentage of the severity, it is shown that Hambantota division has the highest magnitude and it indicates that, this area has a higher vulnerability to degrade with time.

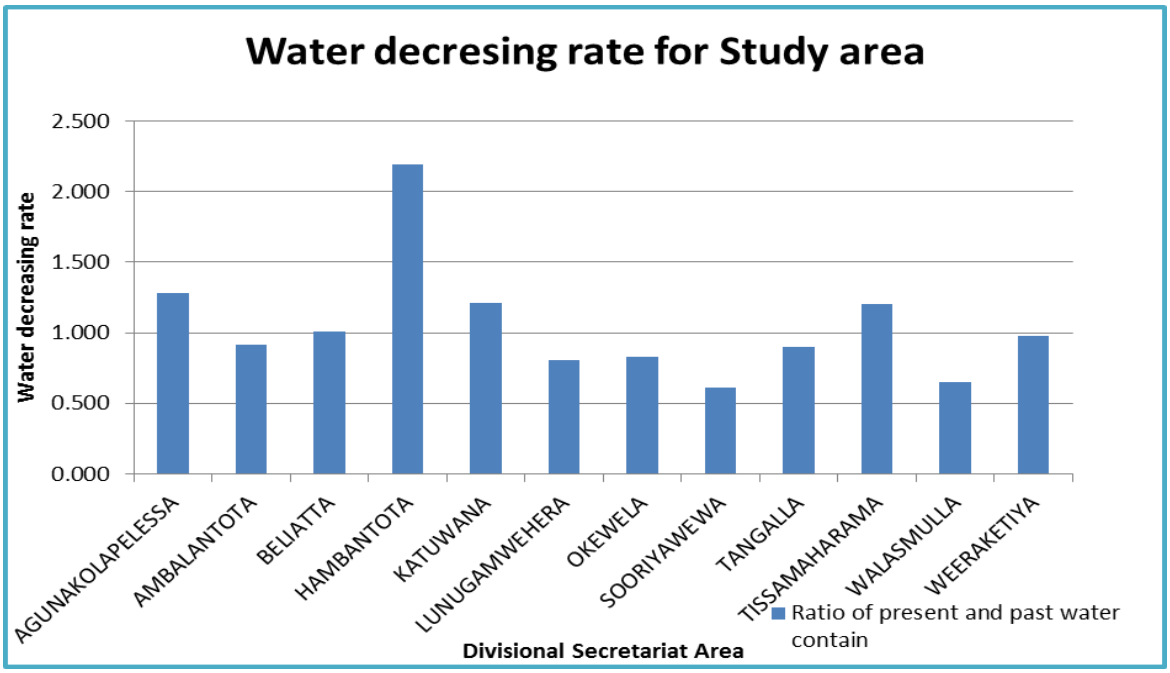

Figure 4-12: Water decreasing rate for study area

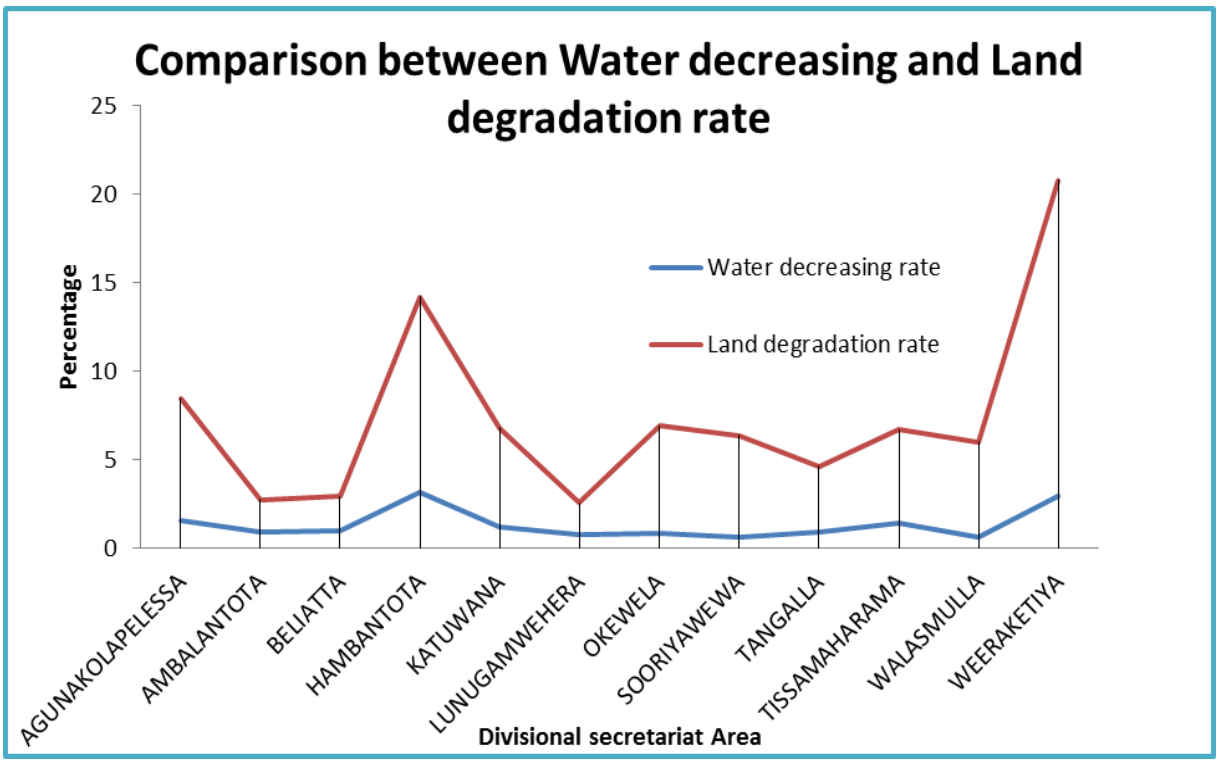

Figure 4-13: Comparison between Land degradation rate and Water decreasing rate

The figure 4-13 shows both quantities show a similar variation pattern. In Hambantota, Agunakolapelessa and Weeraketiya, it is shown that when the land degradation is increasing the decreasing of water contain also increasing depicting a clear relativity between them.

5. Conclusion and Recommendations

5.1. Conclusions

- Increasing land degradation lead to the acceleration of the sensitivity of the land surface to wind erosion and then to formation of dust storms which has negatively serious impact on the environment and public health. Results of this study confirm that integration of GIS and Remote Sensing is suitable for identifying the land degradation, degradation increment patterns, their trends and its consequences in an area.

- The results of this study show clearly and unequivocally the state of land degradation experienced by the studied areas in the Hambantota District of Sri Lanka. It highlighted the need to develop plans to protect the mentioned area.

- Overall results of the study indicated a general vegetation deterioration of 8.56%, an increase in the sand dune accumulation by 5.377%, an increase in the build-up area by 3.188%, as well as to the reduction in surface area of water bodies in the region by 30.639 km^2. The land degradation risk in the study area has increased by 32.4091% during the study period.

- Cloud free images increase the accuracy of the results.

- Overall results of the study indicated the land degradation risk in the study area has increased by 333.29% during the study period (8 years).

5.2. Recommendations

- Selected study area is now under a risk of degradation so rehabilitation endeavors should be directed to each and every area, Specially Hambantota divisional secretariat area where a higher degradation is observed.

- For the further studies if used high resolution satellite images with ground truth data that may be illustrate Land degradation efficiently.

References

Ayad M. F., 2009. Land Degradation Detection Using Geo-Information Technology for Some Sites in Iraq. Journal of Al-Nahrain University, Vol.12 (3), September, 2009, pp. 94-108.

Abu Sayeed, 2014, Causes and Consequences of Land Degradation, Södertörn University | School of Life Sciences.

Brandt TSO, Paul M. Mather, 2000, Classification Methods For Remotely Sensed Data Second Edition, Boca Raton, FL 33487-2742, pp 1 -38.

Gilmore S, Saleem A, Dewan A, 2015, Effectiveness of DOS (Dark-Object Subtraction) method and water index techniques to map wetlands in a rapidly urbanising megacity with Landsat 8 data,, B. Veenendaal and A. Kealy (Eds.): Research@Locate'15, Brisbane, Australia.

Hanqiu X., 2006, Modification of normalized difference water index (NDWI) to enhance open water features in remotely sensed imagery, College of Environment and Resources, Fuzhou University; Key Laboratory of Data Mining and Sharing, China's Ministry of Education; Fuzhou, Fujian 350002, China.

Higginbottom T.P., Symeonakis E., 2014, Assessing Land Degradation and Desertification Using Vegetation Index Data: Current Frameworks and Future DirectionsRemote sensing ISSN 2072-4292.

Hua Li, Qinhuo Liu , 2014, Comparison of NDBI and NDVI as indicators of surface urban heat island effect in MODIS imagery, Institute of Remote Sensing Applications of Chinese Academy of Sciences and Beijing Normal University, Beijing 100101, China.

Mohammed F.A., 2016, Sand dunes monitoring using remote sensing and GIS techniques for some sites in Iraq, Proceedings of SPIE - The International Society for Optical Engineering.

Nath B, 2014, Quantitative Assessment of Forest Cover Change of a Part of Bandarban Hill Tracts Using NDVI Techniques, Journal of Geosciences and Geomatics, 2014, Vol. 2, No. 1, 21-27.

Pat S. Chavez, JR, 1988, an improved dark-object subtraction technique for atmospheric scattering correction of multispectral data, https://www.researchgate.net/publication /223795843.

Project Report N°L-10, 2009, LAND DEGRADATION ASSESSMENT AND RECOMMENDATION FOR A MONITORING FRAMEWORK IN SOMALILAND.

Sri Lanka National Report on Disaster Risk, Poverty and Human Development Relationship, 2009, Disaster Management Centre United Nations Development Programme in Sri Lanka United Nations Development Programme Regional Centre, Bangkok.

Stuart K. McFeeters, 2013, Using the Normalized Difference Water Index (NDWI) within a Geographic Information System to Detect Swimming Pools for Mosquito Abatement: A Practical Approach, Department of Geography, California State University Fresno, Fresno 2555 E. San Ramon Ave, MS SB69, Fresno, CA 93740, USA.

Tejaswi G, March 2007 , Manual On Deforestation, Degradation, And Fragmentation Using Remote Sensing And Gis, Strengthening Monitoring, Assessment And Reporting On Sustainable Forest Management In Asia (Gcp/Int/988/Jpn), pp 5-6.

Vyjayanthi N., Jha C. S., Murthy M. S. R., Yadav D.K., Singh L. October, 2008, Forest Biomass Estimation and Forest Structure Analysis of Deciduous Forests Using SAR Data, Indian Space Research Organisation, Hyderabad ,pp 1 -14.

Yahaya Z., Balzter H., Jörg ,Tucker C. J.,2015, Land Degradation Assessment Using Residual Trend Analysis of GIMMS NDVI3g, Soil Moisture and Rainfall in Sub-Saharan West Africa from 1982 to 2012, Remote sensing ISSN 2072-4292.